processes

MDPI

Article

Experimental Development of Coal-Like Material with Solid-Gas Coupling for Quantitative Simulation Tests of Coal and Gas Outburst Occurred in Soft Coal Seams

Xingkai Wang [1,2,*], Wenbing Xie [1,*], Zhili Su [2] and Qingteng Tang [2]

[1] State Key Laboratory of Coal Resources and Safe Mining, China University of Mining and Technology, Xuzhou 221116, China

[2] School of Mines, China University of Mining and Technology, Xuzhou 221116, China; suzhili1991@163.com (Z.S.); tangqingteng@126.com (Q.T.)

* Correspondence: tb16020019b2@cumt.edu.cn (X.W.); 1692@cumt.edu.cn (W.X.); Tel.: +86-183-5134-3101 (X.W.); +86-139-5220-6989 (W.X.)

Received: 28 January 2019; Accepted: 7 March 2019; Published: 13 March 2019

Abstract: Solid-gas coupling coal-like materials are essential for simulating coal and gas outbursts and the long-term safety study of CO_2 sequestration in coal. However, reported materials still differ substantially from natural coal in mechanical, deformation and gaseous properties; the latter two aspects are common not considered. There is a lack of a definite and quantitative preparation method of coal-like materials with high similarity for future reference. Here, 25 groups of raw material ratios were designed in the orthogonal experiment using uniaxial compression, shearing and adsorption/desorption tests. Experiment results indicated that the coal-like materials were highly similar to soft coals in properties mentioned above. And range analysis revealed the key influencing factors of each mechanical index. The gypsum/petrolatum ratio controls the density, compressive strength, elastic modulus, cohesion and deformation characteristic. The coarse/fine coal powder (1–2 and 0–0.5 mm) controls the internal friction angle and is the secondary controlling factor for compressive strength and elastic modulus. The effect of coal particle size on the sample strength was studied using scanning electron microscope (SEM). When the gypsum/petrolatum ratio increased, the deformation characteristics changed from ductile to brittle. The different failure modes in the samples were revealed. The coal powder content is a key in the gas adsorption/desorption properties and an empirical formula for estimating the adsorption capacity was established. Based on the range analysis of experimental results, a multiple linear regression model of the mechanical parameters and their key influencing factors was obtained. Finally, a composition closely resembling the natural coal was determined, which differs by only 0.47–7.41% in all parameters except porosity (11.76%). Possible improvements and extension to similar materials are discussed. The findings of this study can help for better understanding of coal and gas outburst mechanism and stability of CO_2 sequestration in soft coal seams.

Keywords: tectonically deformed coal; coal and gas outburst; coal-like material; mechanical properties; deformation feature; adsorption/desorption properties

1. Introduction

Coal and gas outburst accidents are among the most serious disasters affecting coal mining [1–4] and a problem in almost all major coal-producing countries [2–4]. Coal and gas outburst is an extremely complex gas dynamic phenomenon, in which large amounts of coal and gas are often ejected at a very

fast rate from the coal rock seam to the mining space in a very short period of time (a few seconds to a few minutes). Such outbursts could destroy underground facilities, damage the ventilation system, cause a large number of casualties and even induce secondary accidents such as gas burning or explosion [2,4–7]. Today, more than half of the disasters due to coal and gas outbursts occur in China [8], causing major economic losses and casualties.

Many factors could cause coal and gas outbursts, including in-situ stress, gas pressure, geological structure, physical and mechanical properties of coal, mining methods and so forth. [6–10]. At present, there is no coherent model that can fully reveal their internal mechanism. In addition, the sudden, transient and dangerous nature makes it almost impossible to observe or study these processes on site. Therefore, simulation tests have been rapidly developed and used to explore the mechanism and process of coal and gas outbursts [5,9,11–15]. However, coal seams that are prone to coal and gas outbursts often have high gas content and low strength and so it is difficult to retrieve samples from the field for large-scale simulation tests. Hence, the development of similar solid-gas coupling coal-like materials in the lab is indispensable for studying the mechanism of coal and gas outbursts.

In addition, there is growing realization in recent years among researchers that coal seams with strong gas adsorption/desorption capacity may be able to capture and store CO_2 [16–21]. However, the key challenge here is the uncertain impact of CO_2 on the mechanical properties of coal and how this will affect the long-term safety and stability of storage. On the other hand, natural coal has extremely complex composition and physical structure, as well as strong heterogeneity–even two samples close to each other in the same coal seam could have significantly different mechanical properties. This seriously hinders the analysis of laboratory test results and the understanding of the above uncertainty. So, homogeneous and reproducible coal-like materials (also called reconstituted coal sample) will provide significant advantages for studies related to CO_2 sequestration in coal.

The key to solve the above two problems is to develop solid-gas coupling coal-like materials that closely resemble the target natural coal in their mechanical and gaseous properties and deformation features. Table 1 lists representative papers on preparing coal-like materials. There are mainly three types of methods. The first is to directly press the coal powder without any added substances [5,12,22]. For example, in 1953, a one-dimensional coal and gas outburst simulation test was completed using briquettes that were cold pressure formed [22]. Skoczylas [12] used fine coal powder to produce a series of briquettes (40 mm in diameter, 110 mm in height and with porosities of 11.2–32.0%) and the test results indicated that they had similar gaseous characteristics to natural coal. However, the coal samples prepared by only molding pressure had very low strength. The second type is pressing coal powders with water, oil or diesel but without any binder [11,20,23–27]. Jasinge et al. [20] prepared reconstituted brown coal sample by compacting 0–1 mm coal particles, in order to study the effect of coal swelling on its permeability in the laboratory. While there was a marked similarity in permeability between natural brown coal and reconstituted specimens, the strength of this type of briquette sample was still lower than natural coal and the gas adsorption/desorption characteristics were also quite different. The third type is pressing a powder mixture consisted of coal powder, cement, sand, lime and other substances [6,10,13,18,19,21,28–30]. Hu et al. [13] made coal-like materials using coal powder, cement, water, sand and activated carbon. They studied the effect of the proportion of each component on the density and mechanical properties of the samples. In 2017 and 2018, Wang et al. [10] and Zhao et al. [6] studied the gas and CO_2 adsorption characteristics of such coal-like materials. Zhang et al. [30] analyzed the influence of different material ratios on the elastic modulus. This last type of coal sample and its preparation method represent outstanding progress in the development of coal-like materials. Nevertheless, the deformation characteristics and failure modes of similar materials, which play an important role in the preparation, forming and developing stages during coal and gas outburst [13], are often not considered and rarely compared with those of natural coal. A clear discussion of related researches can be seen in Figure 1.

The abovementioned studies made important contributions to laboratory research on coal and gas outbursts and CO_2 sequestration. However, at present, there are still the following problems in the development of coal-like materials:

(1) The coal powders used in existing literature have different particle size and molding pressure, molding time and additives are also different. In future simulation test, repeated adjustments are usually needed to determine a suitable proportion of materials. There is still a lack of definite and quantitative preparation method of coal-like materials for future reference.

(2) The similarity remains low between coal-like materials and natural coal in mechanical and physicochemical properties, especially in that the former still have lower strength and very few indexes were measured. Their deformation features and adsorption and desorption characteristics are often not considered and still significantly different from those of natural coal [6,10,13,19,29]. As a result, most simulation studies only reported qualitative rather than quantitative results [13,31]. Today, the understanding of coal and gas outburst mechanism remained poor, the predictions were inaccurate and coal and gas outburst accidents still account for a large proportion of accidents in coal mines [14,32,33].

In this study, we propose a systematic and quantitative development method to determine a solid-gas coupling coal-like material that could closely resemble given natural coal in the mechanical properties, adsorption/desorption features and deformation characteristics. First, according to the physical and mechanical parameters of natural coal samples, raw materials were selected, that is, coarse and fine coal powder, gypsum, petrolatum and light calcium carbonate. Second, the orthogonal method was used to design 25 groups of schemes with different raw material ratios. Meanwhile, the sample preparation method was optimized to improve the homogeneity and reproducibility. Then, density, uniaxial compressive strength (UCS), elastic modulus (EM), cohesion, internal friction angle (IFA), deformation and failure modes, porosity and adsorption/desorption characteristics of samples were tested. Third, range analysis revealed the key influencing factors of each mechanical and physicochemical index and the levels of influence of each factor on a given index. A multivariate linear model was proposed to predict the mechanical parameters of the materials. Fourth, the effects of different particle sizes on the sample strength were examined by scanning electron microscope and the effects of gypsum/petrolatum ratio on the deformation evolution of samples were also analyzed. Finally, a material ratio scheme closely resembling the natural coal was identified. Related improvements and remaining problems in the preparation of similar material were also discussed. This study would contribute to the prevention and control of coal and gas outbursts, as well as other physical simulation tests related to soft coal seams.

Table 1. Representative literature methods for preparing coal-like materials.

No.	Coal Particle Size (mm)	Compaction Pressure (MPa)	Additives	Molding/Air Curing Time (h)	References
1	0–0.2	2.76–19.90	None	-	[5,12,22]
2	0.25–0.38	100	Water	Molding curing 0.33 h	[23–25]
3	0–1	4–13	Water	Molding curing 24 h	[20]
4	0.18–0.25	100	water	24 h drying in drying basin	[11]
5	0.18–0.25	100	Water	Molding curing 0.5 h	[26]
6	0–1.7	4	Water	-	[27]
7	0.1–1	5.7	Cement, water	Molding curing 24 h, air curing 96 h	[18,28]

Table 1. *Cont.*

No.	Coal Particle Size (mm)	Compaction Pressure (MPa)	Additives	Molding/Air Curing Time (h)	References
8	0–0.8	2–6	Cement, water	Molding curing 14.6–20 h, air curing 96–24 × 28 h	[19]
9	0.063–1	5	Phenol-Formaldehyde Resin, potassium hydroxide alkaline aqueous, distilled water	Molding curing 3–26 h, air curing time 144.5–598.5 h	[21]
10	0.18–0.25	100	Cement, water	Molding curing 0.17 h, air curing 24 × 28 h	[29]
11	0.18–0.38/0.38–0.83 mass ration 1:1	25	Cement, sand, activated carbon, water	Air cured 7 × 24 h	[6,10,13]

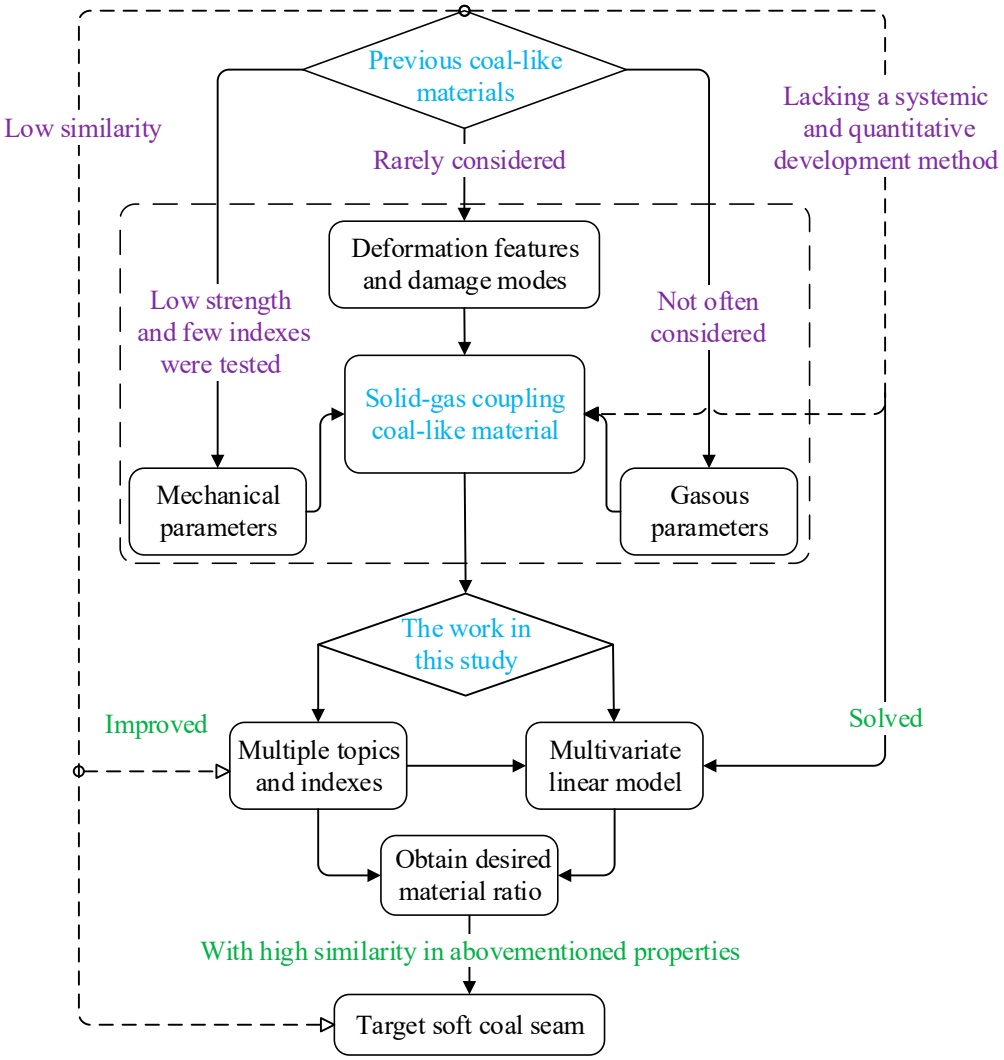

Figure 1. The difference between this work and the previous studies.

2. Materials and Methods

2.1. Preparation and Testing of Natural Coal Samples

Studies have shown that most of the coal and gas outburst occur in tectonically deformed coal (TDC) [34–36]. This is mainly because TDC is formed under mono- or multi-phase strong tectonic movements. Its original structure has been deformed or damaged, resulting in larger adsorption surface area and higher gas content than the primary coal [37]. In this paper, the natural coal samples were selected from a typical tectonically deformed coal seam from No. B-1 Coalbed, Zhengzhou, Western Henan, China, where there have been frequent coal and gas outburst disasters over the last 60 years [7]. According to the new structural-genetic classification system [38], the TDC samples belong to medium-rank and mylonitic structure coal and are characterized by low strength and strong gas adsorption/desorption [32].

Because this coal seam is soft and fragile, it is difficult to obtain large samples using the traditional drill core sampling method. The natural coal standard samples were obtained successfully only after many attempts and improvements. Specifically, a square iron sampler was used to cut the underground coal seam to obtain a sample of approximately 100 mm × 100 mm × 150 mm and the sample was quickly placed in a sealed bag packaging for preservation. The sample was then carefully polished in the lab using a grinding machine. Samples of two target sizes were prepared: 50 mm × 50 mm × 100 mm for uniaxial compression test and 50 mm × 50 mm × 50 mm for variable angle compression shear test. The sample standard requirements and test procedures are in accordance with methods for determining the physical and mechanical properties of coal and rock (Part 7 [39] and Part 11 [40]). The sample loading rate was 0.5 mm/min. The basic physical and mechanical parameters of coal sample are as follows: apparent density =1.280 g/cm^3, UCS = 1.72 MPa, elastic modulus = 126.35 MPa, cohesion = 0.17 MPa and internal friction angle = 27°. However, the success rate of natural coal sample preparation remained only approximately 5%. The proximate analysis results of this TDC are as follows: moisture content Mad = 0.95%, ash content Ad = 10.42%, volatile matter content Vad = 13.95%, porosity = 15.3%, gas adsorption constants a = 39.789 and b = 1.113 and index of initial velocity of gas diffusion Δp = 26–29.

The stress-strain curve in Figure 2 contains the typical stages of initial compaction, linear elastic deformation, strength hardening and softening. Notably, it includes a longer compaction phase than primary coal seam, as well as a plastic or shearing deformation stage. The peak-failure strain of TDC reached 1.73%, which was significantly larger than those of brittle coal or rock (approximately 0.5%) [41]. In addition, microstructure test (Figure 3) showed that the coal body was very broken. The original structure was almost completely destroyed and was composed of particles of different sizes and the texture was loose. This was the reason why the density and strength of TDC were both usually smaller than those of the primary coal seam.

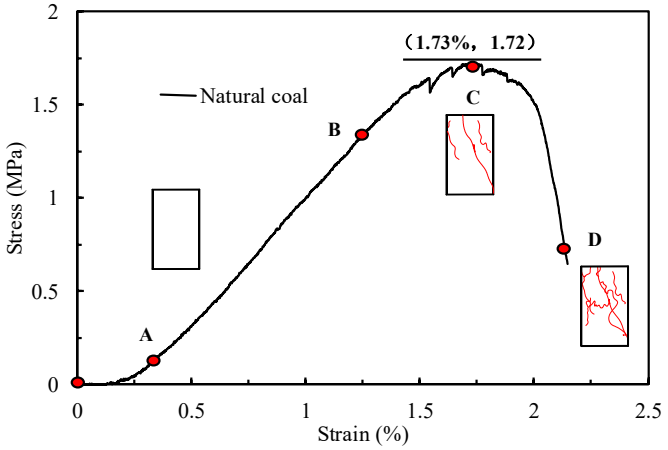

Figure 2. The stress-strain curve of target natural coal.

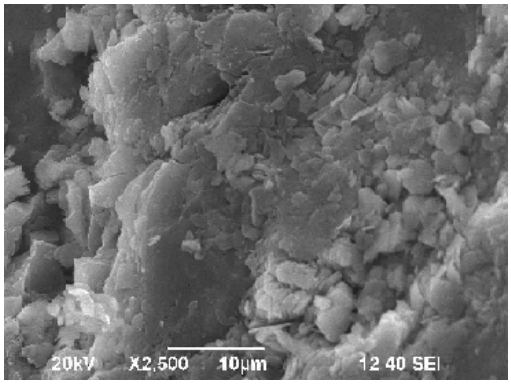

Figure 3. The structure of natural coal under scanning electron microscope.

2.2. Similarity Criteria and Index

Coal and gas outburst is a complex solid-gas coupling process. The currently accepted view is that it is mainly caused by the combined action of in-situ stress, gas pressure and physical and mechanical properties of coal [7–10]. The coal and gas outburst consists of three successive stages [13], among which the static deformation and failure of coal occur during the important outburst preparation stage, while the fracturing of gaseous coal and the movement of pulverized coal and gas occur during the forming and developing stage. Therefore, several similarity criteria (C_i in Equation (1) below) have been proposed to describe the whole process of coal and gas outburst, by using mechanical, deformation and energy models and considering the experimental conditions [6]:

$$\begin{cases} C_\gamma = C_n = C_\varphi = C_p = 1 \\ C_\sigma = C_E = C_c = C_l C_\gamma \end{cases} \quad (1)$$

where γ, n, φ, p, σ, E, c and l, are the volumetric weight, porosity, internal friction angle, gas pressure, compressive strength, elastic modulus, cohesion and length, respectively.

Judging from the above, the similarity index of the coal-like materials should include the physical and mechanical parameters (density, uniaxial compressive strength, elastic modulus, internal friction angle, etc.) and deformation properties and failure mode, as well as porosity, absorption constants (a, b) and desorption index (Δp) of the initial gas diffusion velocity.

2.3. Preparation of Coal-Like Material Samples

2.3.1. Composition Selection

Coal-like materials generally consist of aggregates, binders and additives. The raw materials should be selected according to the following principles: (1) similar to the natural coal material, (2) abundant and low-cost and (3) safe, non-toxic and environment-friendly. In the coal and gas outburst tests [6], the density of coal-like material should be the same as that of natural coal. So, the natural coal powder was selected as the aggregate. Another important reason for using coal powder was that it had good adsorption characteristics similar to the natural coal. However, the particle sizes of coal powders reported in Table 1 were different. Some studies [30,42] have shown that larger coal particles (greater than 3 mm) would undergo secondary crushing during the molding and pressing process, which would have an adverse effect on molding. Therefore, two types of coal powders with particle sizes of 1–2 mm and 0–0.5 mm were used respectively as the coarse and fine aggregates. The fine coal powder was the main aggregate to ensure the molding quality. Second, the binder was selected. Normally, the binder has the greatest influence on the strength and deformation parameters of the material. As the strength of sample obtained by pressing only coal powder was too low, gypsum was selected to adjust the strength parameters of coal-like materials. Portland cement was not used here, because the cement hardening time was too long (more than 28 days). Its strength would also change with

time, which could lead to strength instability of coal-like materials [19] and poor homogeneity and reproducibility. On the other hand, petrolatum was selected to adjust the deformation characteristics of the coal-like materials.

The molding pressure has an important effect on the density and porosity of briquette [5,12]. Excessive molding pressure would damage aggregates with large particle size and affect the molding quality. Therefore, the molding pressure was designed based on the ground stress level of the coal seam. The vertical stress level of the coal seam was approximately 7.2 MPa. In addition, in order to allow the gypsum to play a bonding role, it was necessary to add an appropriate amount of water. After repeated tests, it was found that when the moisture exceeded 11%, the material was too wet and would affect the molding, while the raw material to water ratio of 10:1 was relatively reasonable. Because the density of gypsum (2.3 g/cm^3) is higher than that of natural coal, it was also necessary to use minuteness super white light calcium carbonate with very stable mechanical properties to match the target density while using different material ratios. The selected material compositions are shown in Table 2 and Figure 4.

Table 2. Selected raw materials.

Type	Name	Remarks
Aggregate	Coal powder	1–2 mm and 0–0.5 mm coal particles
Binder	Gypsum (The Group of TZU She Tang Gypsum, Taiwan, China)	Particle size 0.048 mm, density 2.3 g/cm^3, fast-hardening for 15–45 min
	Petrolatum (Dezhouchengze Co., LTD, Dezhou, in Shandong Province, China)	Medical grade, density 0.83 g/cm^3
Auxiliary material	Light Calcium carbonate (Darui Chemical Co., LTD, Gaoan, in Jiangxi Province, China)	Ultra-fine, ultra-white, light calcium carbonate, 0.1 μm < particle size ≤ 1 μm, stable performance, density 0.54 g/cm^3
Water		Tap water

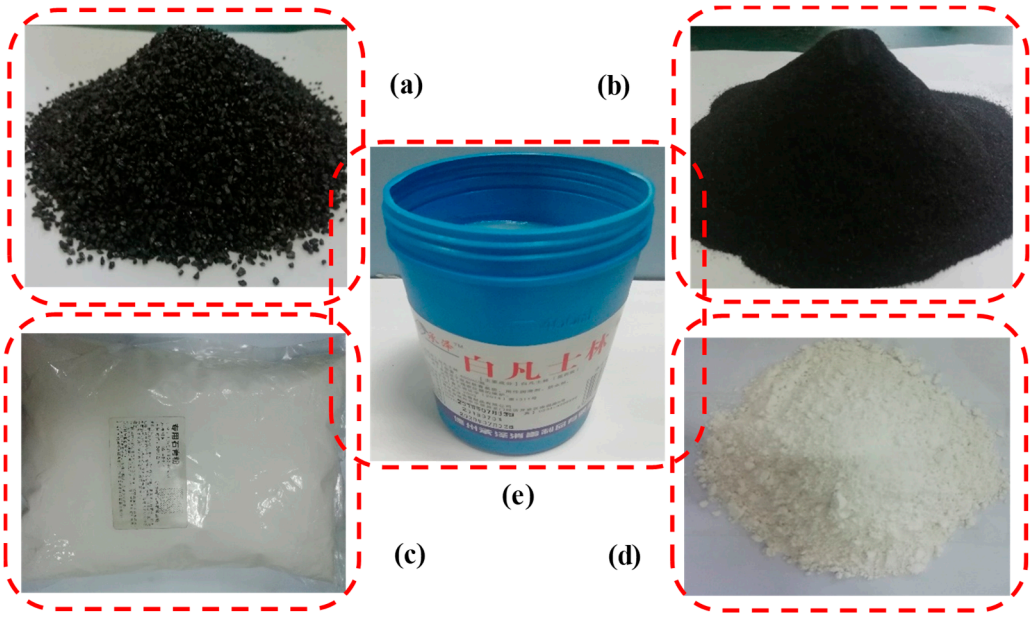

Figure 4. Photographs of the components. (**a**) The coarse aggregate, (**b**) fine aggregate, (**c**) gypsum, (**d**) Minuteness super white light calcium carbonate powder and (**e**) petrolatum.

2.3.2. Design Scheme

The components and their ratios both have an impact on the physical and mechanical properties of coal-like materials. The orthogonal test method was used to design 25 groups of ratios, as shown in Tables 3 and 4. The advantage of this method was that the schemes included a combination of any two factors at all levels and reduced the amount of experimental work [43].

Table 3. The 4 factors and 5 levels of the orthogonal test design.

Level \ Factor	A-Aggregate/Binder	B-Coarse/Fine Aggregate	C-Gypsum/Petrolatum	D-Calcium Carbonate (%)
1	6:1	1:9	5:5	2
2	7:1	2:8	6:4	3
3	8:1	3:7	7:3	4
4	9:1	4:6	8:2	5
5	10:1	5:5	9:1	6

Table 4. The 25 groups of material composition ratio schemes.

Group No. \ Factor	Aggregate/Binder	Coarse/Fine Aggregate	Gypsum/Petrolatum	Calcium Carbonate (%)
1	6:1	1:9	5:5	2
2	6:1	2:8	6:4	3
3	6:1	3:7	7:3	4
4	6:1	4:6	8:2	5
5	6:1	5:5	9:1	6
6	7:1	1:9	6:4	4
7	7:1	2:8	7:3	5
8	7:1	3:7	8:2	6
9	7:1	4:6	9:1	2
10	7:1	5:5	5:5	3
11	8:1	1:9	7:3	6
12	8:1	2:8	8:2	2
13	8:1	3:7	9:1	3
14	8:1	4:6	5:5	4
15	8:1	5:5	6:4	5
16	9:1	1:9	8:2	3
17	9:1	2:8	9:1	4
18	9:1	3:7	5:5	5
19	9:1	4:6	6:4	6
20	9:1	5:5	7:3	2
21	10:1	1:9	9:1	5
22	10:1	2:8	5:5	6
23	10:1	3:7	6:4	2
24	10:1	4:6	7:3	3
25	10:1	5:5	8:2	4

2.3.3. Sample Preparation Method

(1) The raw materials were weighed accurately using an electronic scale according to the given ratios based on a total amount of 1000 g. (2) The dry components (coal powder, gypsum powder and calcium carbonate powder) were mixed and stirred uniformly. (3) A mixture of water and petrolatum was heated to 45 to 50 °C to melt it into a liquid and then quickly mixed with the materials. (4) The well-mixed coal-like materials were divided into five equal parts by weight and put into the mold. Each layer was pressed by a servo press machine at the speed of 120 mm/min. The target pressure was 14.137 kN (the calculated stress was 7.2 MPa) and the load was maintained for 10 s. The actual load-time curve during the layer-by-layer compaction press is shown in Figure 5a. Finally, the whole sample was compacted by the press at the molding pressure of 7.2 MPa and maintained for 10 min, mainly to make the overall force on the whole sample consistent. The loading path on the whole sample can be seen in Figure 5b. It should be noted that the surface between two adjacent layers

should be roughened before filling in the next layer of material to increase the adhesion between layers. The steel mold had an inner diameter of 50 mm, a height of 120 mm and a wall thickness of 10 mm. The mold was approximately 20 mm higher than the sample, making it convenient for the fifth material to be added to the mold at one time. The inner surface of the mold had to be very smooth to reduce the friction. (5) With a self-designed demolding device, as shown in Figure 5d, the molded sample was pushed out at a speed of 5 mm/min by a press. The sample slowly entered the hollow steel pipe (wall thickness 10 mm, height 200 mm, inner diameter 100 mm, with soft material placed on the bottom to prevent sample damage). Then, the sample was cured at room temperature for 10 to 15 days. The water content was tested continuously in this process. When the water content was the same as that of the natural coal, the sample was sealed and stored in a plastic bag in time. In particular, it should be pointed out that many reconstituted coal samples were destroyed during the extrusion process in the past [18], while by using the designed demolding method here, the success rate of sample preparation was 100%. The use of a press machine with quantitative loads for compacting the materials was also an improvement over the manual pressing used in previous studies, which was difficult to quantify and lowered the homogeneity and reproducibility of samples.

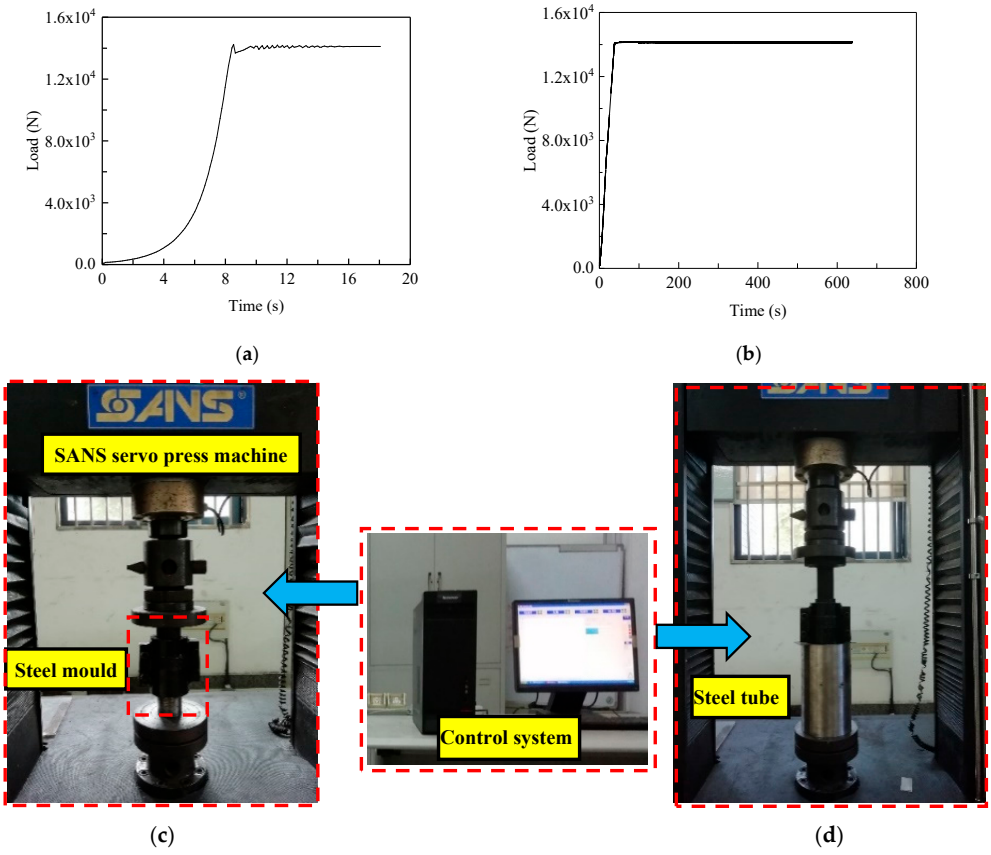

Figure 5. Sample molding and demolding process. (**a**) The load-time curve during the compaction process of each layer of material. (**b**) The load-time curve during the compaction process of the whole sample. (**c**) Sample compression molding process. (**d**) Sample demolding process.

2.3.4. Sample Tests

The sample preparation met the requirements suggested by International Society for Rock Mechanics [44]. The height of the sample was more than twice the diameter. For each group of formulation scheme, 6 samples of Φ 50 mm × 102 mm were made (a total of 150 samples). Two samples in each group were used for the uniaxial compression test (Figure 6a), three were cut into 6 pieces Φ 50 mm × 50 mm in size to perform the variable angle shear tests (Figure 6b). The spare sample would be used in the isothermal adsorption and desorption test.

The CSS-44300 universal testing machine (Changchun testing machine research institute, Changchun, China) with electro-hydraulic servo was used to perform the uniaxial compression and variable angle shear tests. The test steps referred to references [39,40]. The sample loading rate was 0.5 mm/min and the surface unevenness did not exceed 0.2 mm.

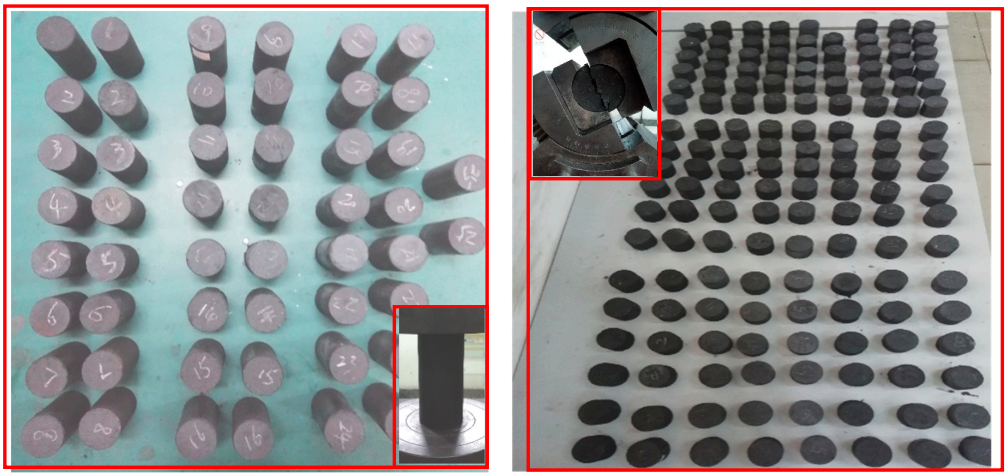

(**a**) (**b**)

Figure 6. Prepared coal-like samples of two sizes: (**a**) Φ 50 mm × 102 mm; (**b**) Φ 50 mm × 50 mm.

3. Result Analysis and Discussion

3.1. Mechanical Properties

3.1.1. Results of Orthogonal Test

The mechanical property test results are shown in Table 5. The property parameters of the 25 groups of coal-like materials covered a wide range: density of 1.171–1.305 g/cm^3, uniaxial compressive strength of 0.55–2.20 MPa, elastic modulus of 32.06–196.18 MPa, cohesion of 0.068–0.248 MPa and the internal friction angle of 16.8–35.6°. These samples could be used for physical simulation of most soft coal seams [13,19].

Table 5. The physical and mechanical parameters of each group.

No.	Density (g/cm^3)	UCS (MPa)	E (MPa)	Cohesion (MPa)	F (°)
1	1.235	0.67	39.76	0.131	17.4
2	1.248	1.24	76.22	0.153	23.8
3	1.251	1.68	91.90	0.192	27.2
4	1.253	1.82	141.45	0.201	32.4
5	1.242	1.74	152.75	0.248	35.6
6	1.228	0.91	35.11	0.132	18.2
7	1.229	1.49	108.22	0.164	20.4
8	1.231	1.94	163.66	0.185	27.8
9	1.296	2.05	181.85	0.203	32.8
10	1.176	0.55	32.06	0.089	28.2
11	1.223	1.16	63.90	0.152	18.7
12	1.289	1.72	111.81	0.173	21.1
13	1.305	2.20	196.18	0.201	30.1
14	1.188	0.89	63.11	0.073	23.7
15	1.184	0.79	49.05	0.095	28.9

Table 5. *Cont.*

No.	Density (g/cm^3)	UCS (MPa)	E (MPa)	Cohesion (MPa)	F (°)
16	1.256	1.39	64.43	0.164	21.6
17	1.252	1.94	163.59	0.213	24
18	1.172	0.99	60.69	0.068	23.4
19	1.171	1.13	84.24	0.089	25.6
20	1.212	1.04	55.07	0.119	29.8
21	1.238	1.61	97.41	0.191	22.4
22	1.181	0.77	49.24	0.061	16.8
23	1.218	1.23	74.83	0.078	22.2
24	1.211	1.38	93.58	0.108	27.4
25	1.209	1.27	77.25	0.128	30.6
TDC	1.280	1.72	126.35	0.17	27

3.1.2. Range Analysis

In addition, according to the orthogonal experimental theory, range analysis (also called visual analysis method) was used to reveal the influence of various factors on results from the orthogonal experiment [43]. That is, the results corresponding to the same level of each factor were averaged and the range was obtained by subtracting the minimum average value from the maximum average value for each level. The range value reflected the influence of different levels of a given factor on the index of interest. A large range indicated that different levels of this factor had strong and different influences on the test results. From the test results in Table 5, the average and range of each level of all factors affecting the density, compressive strength, elastic modulus, cohesion and internal friction angle could be obtained, as shown in Table 6. The effect of different levels of various influencing factors on each index could also be obtained, as shown in Figure 7.

The following observations can be found from Table 6 and Figure 7. (1) For density, the gypsum/petrolatum played the main controlling role. The calcium carbonate content was the secondary factor determining the material density. In Figure 7a, the density of coal-like material increased with increasing gypsum/petrolatum ratio but decreased linearly with increasing calcium carbonate content. (2) For UCS, the gypsum/petrolatum ratio had the highest degree of influence on the compressive strength. The coarse/fine aggregate ratio played a secondary controlling role, followed by the aggregate/binder ratio. Factor D (calcium carbonate content) had almost no influence. In addition, Figure 7b shows that (i) the compressive strength tends to be positively correlated with the gypsum/petrolatum ratio, indicating that increasing the gypsum content could improve the material strength significantly. (ii) The compressive strength first increased then decreased with increasing coarse/fine aggregate ratio, indicating that a reasonable ratio of aggregate particles of different sizes had an important influence on the material strength. When the fine aggregate/coarse aggregate content was approximately 70%, the aggregate had the highest strength. (iii) The compressive strength of coal-like material and aggregate/binder showed a negative correlation. (3) For ***E***, the influence of each factor on the elastic modulus was similar to that on the compressive strength, in the same order of C > B > A > D. (4) For cohesion, the influence of each factor was in the order of C > A > B > D. In Figure 7d, the cohesion of material increased with the increase of gypsum/petrolatum ratio but decreased with increasing aggregate/binder ratios. (5) Regarding IFA, the influence of each factor on internal friction angle was in the order of B > C > A > D. The coarse/fine aggregate had the most significant influence. As shown in Figure 7e, as the coarse aggregate content increased, the internal friction angle increased linearly. This indicated that the friction and bite force between coarse aggregates were significantly larger than those between fine aggregates. Under the condition of ensuring the molding quality, increasing the coarse aggregate content is beneficial to enhancing the internal friction angle of the material.

Table 6. Range analysis of the physical and mechanical indexes.

Level	Average Density (g/cm^3)				Average UCS (MPa)				Average EM (MPa)				Average Cohesion (MPa)				Average IFA (°)			
	A	B	C	D	A	B	C	D	A	B	C	D	A	B	C	D	A	B	C	D
1	1.246	1.236	1.190	1.250	1.43	1.15	0.77	1.34	100.41	60.12	48.97	92.66	0.185	0.154	0.084	0.141	27.28	19.66	21.90	24.66
2	1.232	1.240	1.210	1.239	1.39	1.43	1.06	1.35	104.18	101.82	63.89	92.49	0.155	0.153	0.109	0.143	25.48	21.22	23.74	26.22
3	1.238	1.235	1.225	1.226	1.35	1.61	1.35	1.34	96.81	117.45	82.53	86.19	0.139	0.145	0.147	0.148	24.50	26.14	24.70	24.74
4	1.213	1.224	1.248	1.215	1.30	1.45	1.62	1.34	85.60	112.84	111.72	91.36	0.131	0.135	0.170	0.144	24.88	28.38	26.70	25.50
5	1.211	1.205	1.267	1.210	1.25	1.08	1.91	1.35	78.46	73.23	158.36	102.76	0.113	0.136	0.211	0.147	23.88	30.62	28.98	24.90
Range	0.035	0.035	0.076	0.040	0.18	0.53	1.14	0.01	25.72	57.33	109.39	11.39	0.07	0.02	0.13	0.01	3.40	10.96	7.08	1.56

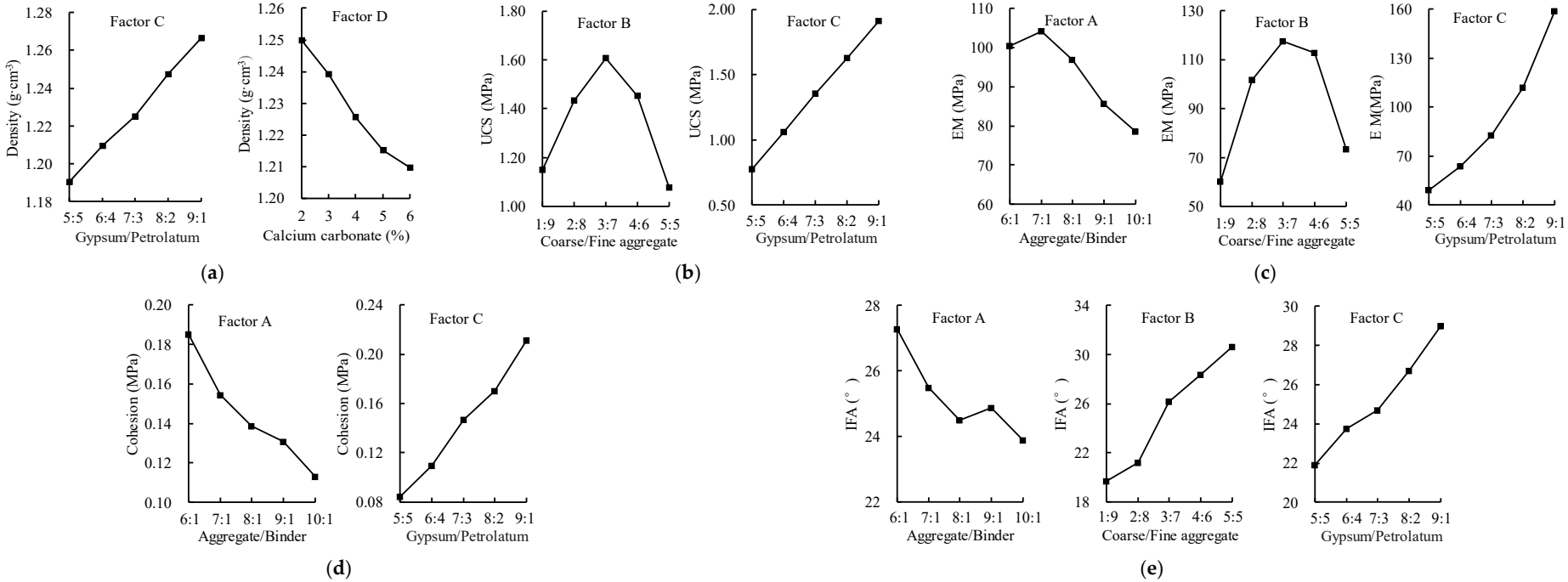

Figure 7. The effect of different levels of key influencing factors on the physical and mechanical indexes: (**a**) density; (**b**) UCS; (**c**) EM; (**d**) cohesion; (**e**) IFA.

3.2. Deformation Characteristics and Failure Modes of the Coal-Like Samples

The range analysis indicated that the gypsum/petrolatum ratio is the main factor affecting the strength indexes of the specimens. Since samples in the 25 groups used in orthogonal uniaxial compression tests showed different deformation processes, it was necessary to study the effect of gypsum/petrolatum ratio on the deformation features. To this end, coal-like materials with aggregate/binder = 6:1, coarse/fine aggregate = 3:7 and gypsum/petrolatum = 5:5, 6:4, 7:3, 8:2 and 9:1 were prepared and used in deformation tests. Figure 8 shows the stress-strain curves of the five types specimens with different levels of gypsum/petrolatum ratios in the uniaxial compression test. All samples contained the typical stages of initial compaction, linear elastic deformation, strength hardening and softening and a residual phase. Samples with low gypsum/petrolatum ratio had lower strength, longer plastic or ductile deformation phase before peak stress and a gentler drop after the peak value. While the sample with gypsum/petrolatum = 9:1 had the greatest strength and shortest plastic deformation phase, the stress declined linearly after the peak to reach a very small residual value, which corresponds to a brittle characteristic.

More importantly, the damage modes of the specimens with different gypsum/petrolatum ratios under uniaxial compression test could be divided into five main types, named as A, B, C, D and E. Figure 9 demonstrates the physical damage modes and corresponding schematic diagrams of the specimens. Type A is squeezing failure, which belongs to ductile damage and occurred in the sample with gypsum/petrolatum = 5:5, that is, a high content of petrolatum. The major features include apparent lateral convex deformation and the lack of obvious large fracture surfaces, as shown in Figure 9(A-1,A-2). Type B is wedge failure, which mainly occurred in the sample with gypsum/petrolatum = 6:4. As shown in Figure 9(B-1,B-2), large wedge-shaped coal blocks slipped from the sample, so that large fissure surfaces could be found in the specimens. Type C is plastic shear failure and mainly occurred in the sample with gypsum/petrolatum = 7:3. This type is characterized by shear cracks and damage everywhere, the absence of obvious large fissure surface, the coal body collapsing in the form of scales and noticeable dilative shear deformation (Figure 9(C-1,C-2)). Type D is brittle shear failure and occurred in the sample with gypsum/petrolatum = 8:2. In this case, first a major fissure appeared and then it propagated and extended through the whole sample. When the sample broke down, there was a large final fracture surface about 45–60° from the specimen axial direction (Figure 9(D-1,D-2)). Type E is brittle splitting failure and occurred in the sample with gypsum/petrolatum = 9:1, that is, high gypsum content. Such samples always split quickly after the peak stress. Figure 9(E-1,E-2) present the ultimate destruction characteristic of type E: one or several vertical cracks ran through the top and bottom of the sample and their directions were approximately parallel to the axis of the specimen.

In addition, the occurrence of coal and gas outbursts must be affected by the deformation and failure mechanism of the coal [13,37]. According to the different deformation mechanisms, different types of TDC are divided into three series of deformation and ten classes, that is, the brittle, the ductile and the brittle-ductile deformation [38]. In this study, upon decreasing the gypsum content or increasing the petroleum content, the deformation of the coal-like materials transitioned from ductile to brittle. The failure modes included typical squeezing damage, wedge splitting, plastic shear failure, brittle shear and brittle fracturing. These varied deformation features are useful in different coal and gas outburst simulation tests.

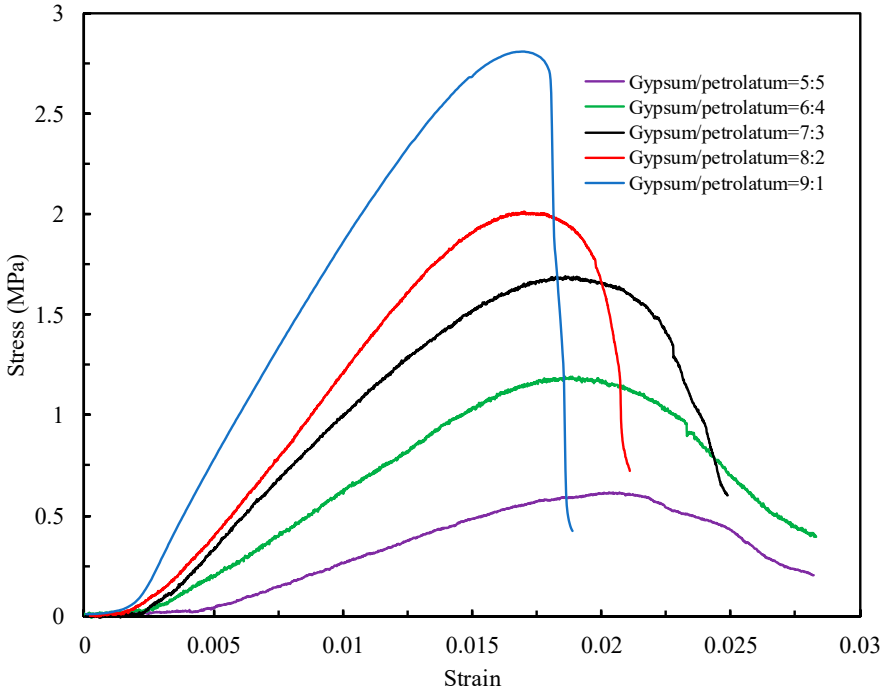

Figure 8. Stress-strain curves of coal-like material specimens with different gypsum/petrolatum ratios.

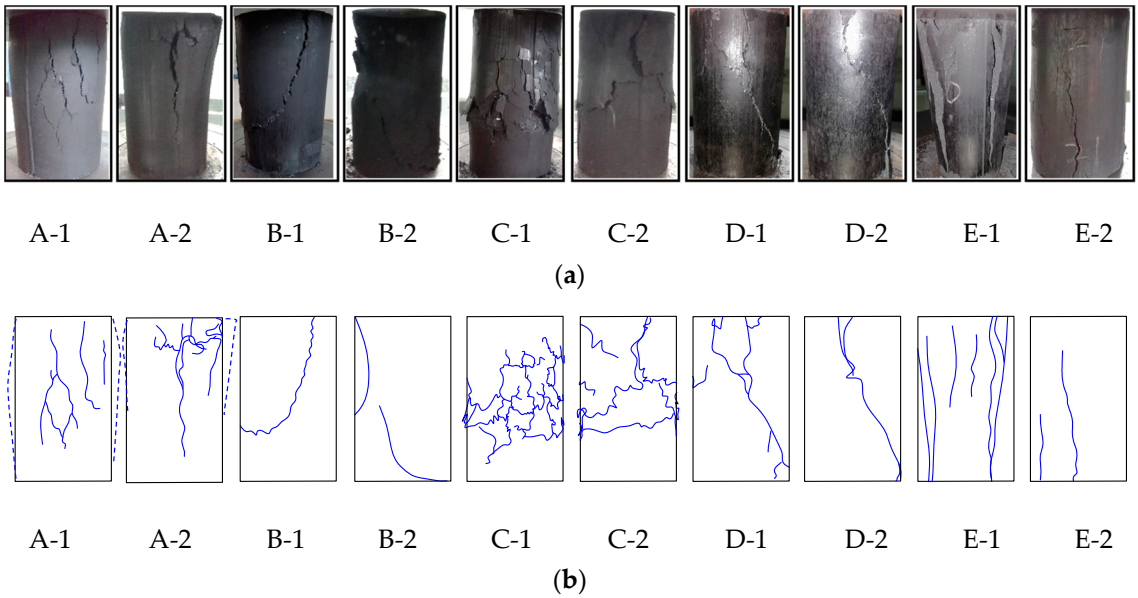

Figure 9. (**a**) The different physical damage modes and (**b**) the corresponding schematic diagrams of the specimens.

3.3. Physicochemical Properties

Samples in the four groups of 4, 8, 12 and 17 had similar mechanical parameters (compressive strength, elastic modulus, cohesion, internal friction angle, etc.) and deformation features to the natural coal. Thus, they were selected for further testing of porosity and gas adsorption/desorption.

3.3.1. Porosity

Porosity refers to the proportion of the volume of pores to the total volume. It can be calculated from the apparent density ρ_a and true density ρ_t of material according to the following equation:

$$k = \frac{1}{\rho_a} - \frac{1}{\rho_t} \quad (2)$$

After the sample was dried, its apparent density could be obtained by weighing using an electronic scale and size measurement using a Vernier caliper. The true density was measured by the automatic industrial analyzer. From the porosity of the three groups of samples (Table 7), it can be seen that their density and porosity were highly consistent with those of the natural coal. So, these coal-like materials could satisfy the porosity and volumetric weight similarity ratio shown in Equation (1) [6]:

Table 7. Porosity of the samples.

Sample	Apparent Density (g/cm^3)	True Density (g/cm^3)	Mass Ratio of Coal Powder (%)	Porosity (%)
TDC	1.268	1.573	-	15.3
No. 4	1.241	1.558	81.43	15.7
No. 8	1.277	1.623	82.25	16.1
No. 12	1.293	1.691	87.11	17.4
No. 17	1.240	1.591	86.40	16.9

3.3.2. Adsorption and Desorption Parameters

The gas adsorption constants a and b, used to quantify the adsorption capacity of coal, were determined by the isotherm adsorption test results using methane of 99.9% purity at 30 °C in combination with the Langmuir equation [6]. The parameter Δp represents the initial velocity of coal gas diffusion [45]. In this paper, the TDC and the samples 4, 8, 12 and 17 were crushed and grains with the particle size of 0.2 to 0.25 mm were sifted out. For each sample group, 6 portions of 3.5 g each were weighed. Each portion was placed in the WFC-2 initial gas diffusion velocity analyzer (Zhengzhou huazhi electronic technology co. LTD, Zhengzhou, China). Air tightness check and vacuum treatment were performed on the test instrument. The gas adsorption and desorption of samples were tested under the conditions of 99.9% pure methane, 0.1 MPa and 20 °C. The averages of the test results are shown in Table 8. It can be seen that the gas adsorption and desorption properties of coal-like materials were consistent with those of the natural coal and could meet the test requirements [6].

Table 8. Adsorption and desorption parameters of samples.

Sample	a (cm^3/g)	b (1/MPa)	Δp (mL/s)
TDC	39.789	1.113	27
No. 4	35.258	1.169	23
No. 8	35.463	1.163	23
No. 12	37.944	1.137	25
No. 17	37.562	1.146	24

Coal has a strong gas adsorption capacity mainly because of its good porosity and relatively large specific surface area [36,37]. Therefore, under the same molding pressure conditions, the coal mass ratio had the most impact on these characteristics. Tables 7 and 8 also verify this feature: the higher the coal content, the larger the porosity of the coal-like materials and the stronger the gas adsorption and desorption capacities. On the other hand, higher contents of gypsum, petrolatum and calcium carbonate reduce the porosity and the methane adsorption/desorption, which is consistent with existing research results [13,46]. Besides, previous results [47] presented that coal particles below 3.35 mm in size have almost no influence on the gas adsorption capacity. Therefore, the

total amount of fine and coarse coal powder can be used to quantitatively estimate the adsorption constants a, as presented in Equation (3) and Figure 10 (with $R^2 = 0.9967$).

$$Y_a = 0.4841X - 4.25 \tag{3}$$

where Y_a is the value of gas adsorption constant a and X is the content of coal powder.

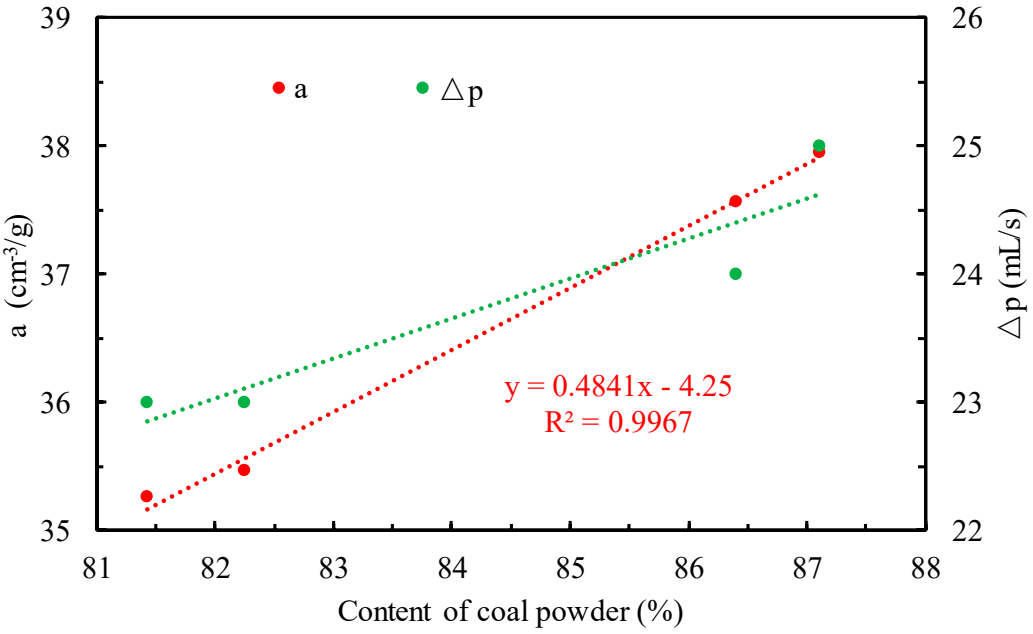

Figure 10. The quantitative relation between coal powder content and the gas absorption constant, a and the desorption index, Δp.

Combining Tables 4 and 7, it can be seen that the four coal-like material groups of 4, 8, 12 and 17 had a coal powder ratio of 81.43 to 87.11%, which almost coincides the overall range for groups 1 to 25 (80.57 to 89.09%). This indicated that the samples in group 1 to 25 all had similar porosity and gas adsorption/desorption characteristics as the natural coal.

3.4. Multivariate Linear Model for Predicting the Mechanical Parameters of Coal-Like Material

According to our range analysis (in Section 3.1.2), each mechanical index has multiple influencing factors. To determine the suitable proportion of materials used in physical simulation, repeated adjustments are usually needed. Thus, results from previous studies can hardly be used directly in future research and it is difficult to promote the rapid development of similar materials. Therefore, it is important to establish a multivariate linear model between the mechanical property indexes and their main influencing factors (as shown in Table 6 and Figure 7). The model can be described by the equations in (4):

$$\begin{cases} Y_{\sigma_c} = C_1 + a_1X_1 + b_1X_2 + c_1X_3 + d_1X_4 \\ Y_E = C_2 + a_2X_1 + b_2X_2 + c_2X_3 + d_2X_4 \\ Y_C = C_3 + a_3X_1 + b_3X_2 + c_3X_3 + d_3X_4 \quad (0 \le X_1, X_2, X_3, X_4, X_5 \le 100) \\ Y_F = C_4 + a_4X_1 + b_4X_2 + c_4X_3 + d_4X_4 \\ Y_D = C_5 + a_5X_1 + b_5X_2 + c_5X_3 + d_5X_4 + e_1X_5 \end{cases} \tag{4}$$

where C_i, a_i, b_i, c_i, d_i and e_i (I = 1, 2, 3, 4, 5) are the fitting constants. The contents of coarse aggregate, fine aggregate, gypsum, petrolatum and calcium carbonate were set as X_1(%), X_2(%), X_3(%), X_4(%) and X_5(%); and the indexes of compressive strength, elastic modulus, cohesion, internal friction angle and density were Y_{σ_c}, Y_E, Y_C, Y_F and Y_D, respectively.

It should be noted that in Figure 11, the elastic modulus of the material increased exponentially (with an excellent correlation of $R^2 = 0.9144$) against the compressive strength, which is consistent with previous studies [13]. More importantly, their similarity ratios are the same in the similarity criteria (as shown in Equation (1)). Therefore, Equation (4) could be simplified to (5),

$$\begin{cases} Y_{\sigma_c} = C_1 + a_1X_1 + b_1X_2 + c_1X_3 + d_1X_4 \\ Y_C = C_2 + a_2X_1 + b_2X_2 + c_2X_3 + d_2X_4 \quad (0 \le X_1, X_2, X_3, X_4, X_5 \le 100) \\ Y_F = C_3 + a_3X_1 + b_3X_2 + c_3X_3 + d_3X_4 \\ Y_D = C_4 + a_4X_1 + b_4X_2 + c_4X_3 + d_4X_4 + e_1X_5 \\ 100 = X_1 + X_2 + X_3 + X_4 + X_5 \end{cases} \tag{5}$$

Then, according to the orthogonal test result in Table 5, the multivariate Equation (5) were fitted using Origin program to identify the regression Formula (6). The R^2 values of Y_{σ_c}, Y_C, Y_F and Y_D were 0.838, 0.965, 0.945 and 0.937, respectively.

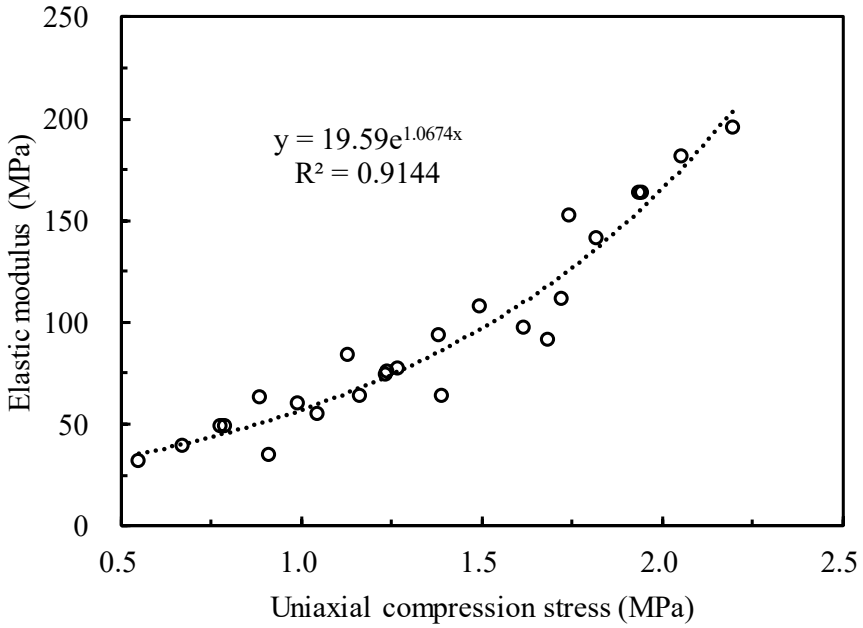

Figure 11. Relationship between modulus of elasticity and uniaxial compressive strength of samples.

$$\begin{cases} Y_{\sigma_c} = 0.01356X_1 + 0.0171X_2 + 0.1305X_3 - 0.13143X_4 - 0.58773 \\ Y_C = -0.0016X_1 - 0.00073X_2 + 0.02122X_3 - 0.00695X_4 + 0.08933 \quad (0 \le X_1, X_2, X_3, X_4, X_5 \le 100) \\ Y_F = 0.27831X_1 - 0.05061X_2 + 1.15883X_3 - 0.40811X_4 + 13.57658 \\ Y_D = -0.00024X_1 + 0.00083X_2 + 0.01278X_3 - 0.00487X_4 - 0.01045X_5 + 1.14431 \\ 100 = X_1 + X_2 + X_3 + X_4 + X_5 \end{cases} \tag{6}$$

According to the physical and mechanical parameters of the raw coal, the five-variable primary equations can be solved using the Mmult and Minverse functions in the Excel program to obtain the corresponding composition (26.6% coarse aggregate, 62.2% fine aggregate, 8.5% gypsum, 1.7% petrolatum and 1% calcium carbonate). The gas absorption capacity of this material was estimated by Equation (3) to be $a = 38.738$.

Then, samples were made according to the determined composition and their indexes were tested in the same conditions. Table 9 shows the differences of each index of mechanical, deformation and gaseous properties between the natural coal and developed coal-like material. The difference in mechanical and gas adsorption/desorption parameters was very small (approximately 0.47 to 11.76%). Figure 12 is the stress-strain curve of the coal-like material, showing evolution characteristics of strength

and deformation (comprehensive damage mode of brittle shearing and plasticity) very consistent to that of the natural coal.

Table 9. Difference analysis between natural coal and determined coal-like material.

Sample	Apparent Density (g/cm^3)	UCS (MPa)	EM (MPa)	Cohesion (MPa)	IFA (°)	Porosity (%)	*a*	Δ*p*
Coal-like material	1.286	1.78	131.85	0.18	25.8	17.1	38.343	25
TDC	1.280	1.72	126.35	0.17	27	15.3	39.789	27
Difference (%)	+0.47	+3.49	+4.35	−5.9	−4.44	+11.76	−3.63	−7.41

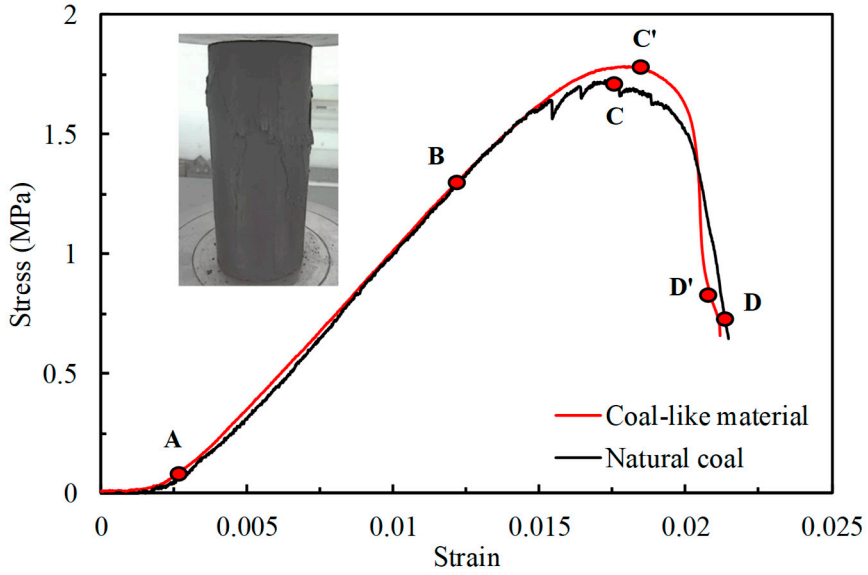

Figure 12. The stress-strain curves of coal-like material and natural coal.

3.5. Discussion

3.5.1. Microscopic Analysis of the Effect of Pulverized Coal Particle Size on Sample Strength

As stated in Section 3.1.2, a reasonable ratio of aggregate particles of different sizes has an important influence on the material strength and elastic modulus. Meanwhile, the particle sizes of coal powders reported in Table 1 were different. To study the effect of particle size on the preparation and strength of samples, coal-like materials with aggregate/gypsum = 10:1, coarse (1–2 mm)/fine (0–0.5 mm) coal particles = 1:9, 3:7 and 5:5 were prepared. Their microstructures were examined by SEM (Figure 13).

On the one hand, the morphology diagrams (Figure 13a) of the three cut specimens show that, when the proportion of fine aggregate was high (coarse/fine coal particles = 1:9 and 3:7), the sample was relatively flat in morphology and relatively dense in structure, while a high proportion of coarse aggregate (coarse/fine coal particles = 5:5) resulted in an uneven sample morphology, a looser structure and a low strength (shown in Figure 7b). On the other hand, in specimen No. 1 shown in Figure 13b, the gypsum (needle shapes) were stuck together when 90% of the coal had a particle size of 0–0.5 mm. This indicates that too much fine coal particles makes it difficult to mix the sample evenly with the cementing agent, resulting in poor strength stability and low homogeneity of the sample, which will have an important impact on the analysis of test results. However, in specimen No. 3 the gypsum was uniformly attached to the surface of coal particles and the very small coal particles were also firmly bonded to the larger ones. Therefore, a large proportion of coarse coal particles is beneficial to the

uniform distribution of cementing agent. When the ratio of coarse/fine coal particles was about 3:7, the cement and aggregate were well mixed, and the specimen also had a compact structure.

In addition, it can be seen that gypsum with its extremely small particle size may reduce the gap between particles and the porosity would be reduced to a certain extent, which helps to reduce the permeability of reconstituted coal.

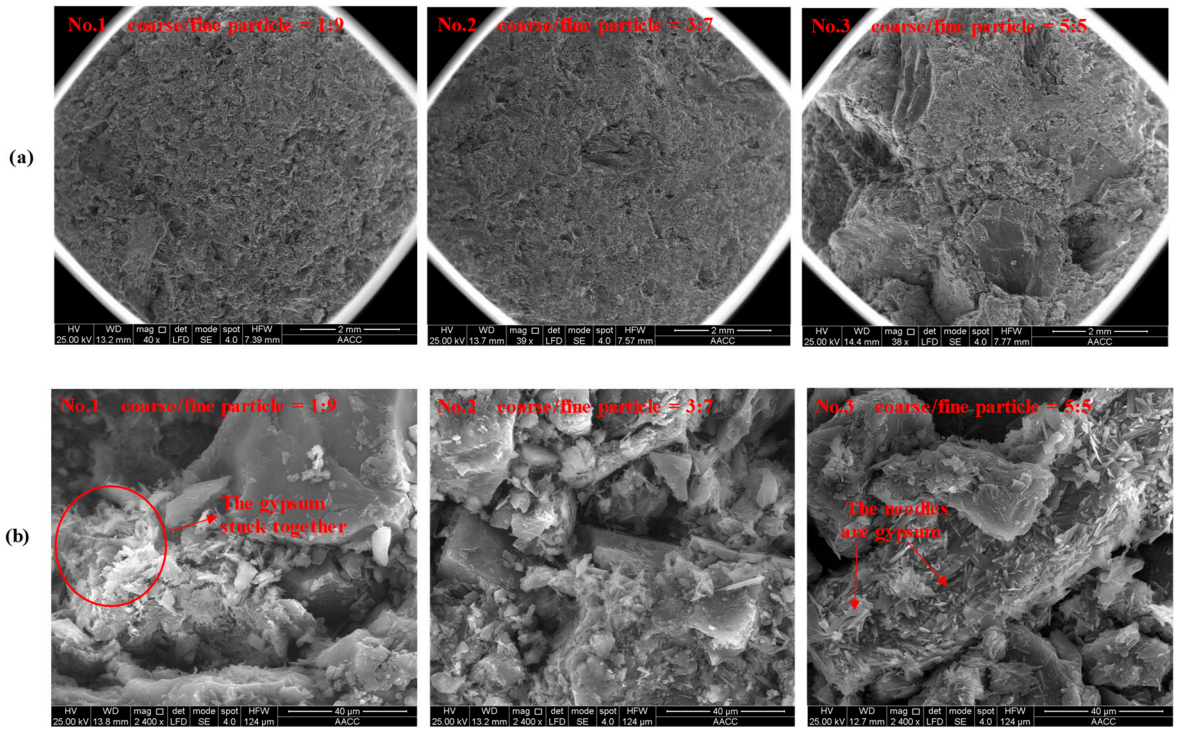

Figure 13. SEM images of three specimens composed with different coarse/fine coal particle ratios: (**a**) the morphology diagrams and (**b**) internal structures of the three cut specimens.

3.5.2. Optimization of Sample Preparation Method and Deformation Characteristic Controlling Binder

Samples made by directly pressing the coal powder have lower strengths larger deformation than the natural coal. Consequently, studies in the past [10,13,18,19,21,29] usually used Portland cement to improve the strength of coal-like materials. However, the mechanical properties of cement keep changing over time. The molding and air curing time (usually 28 days) also have significant influence on the mechanical strengths of the sample and should be considered as additional influencing factors in the preparation process. As a result, the sample preparation process becomes more complex, which makes it hard to ensure the homogeneity and reproducibility. In order to solve this problem, this study used gypsum instead of cement and improved the sample preparation method as discussed in Section 2.3.3 (i.e., using quantitative compaction samples and self-designed molding and demolding equipment). However, gypsum as a binder is less effective than cement in improving the mechanical parameters of materials and so it is more suitable for the preparation of low-strength (0 to 2.5 MPa) coal-like materials. More importantly, gypsum and petrolatum were selected as the compound binder to adjust the deformation characteristics of coal-like materials. Similar materials with ductile to brittle deformation features could be obtained by adjusting the mass ratio of gypsum/petrolatum.

3.5.3. Porosity Adjustment Method

Among the properties summarized in Table 9, the porosity difference was large (11.73%) while the difference in adsorption and desorption parameters was smaller (3.63–7.41%). This indicated that the specific surface area was not very different between the natural coal and coal-like material. Rather, the gap between particles was larger in the coal-like materials. Studies have shown that the porosity of

coal-like materials decreases with increasing molding pressure [12,48]. Thus, the porosity could be adjusted by changing the molding pressure slightly but it could not be reduced by adding inorganic matter. For example, sand will decrease the coal powder content and gas adsorption/desorption capacity and the latter is the most important index in coal and gas outburst simulation tests [6].

3.5.4. Limitation and Future Direction to Improve the Similarity of Solid-Gas Coupling Coal-Like Materials

It can be seen from Table 9 that the difference in gaseous parameters between coal-like material and natural coal was larger than that that in the mechanical parameters. This was mainly because the coal-like material contained inorganic matters (gypsum and calcium carbonate) and petrolatum that do not have gas adsorption properties. Future new binders that could simultaneously increase the strength and adsorption characteristics of coal-like materials will further improve the similarity and broaden the application prospects.

3.5.5. Application Prospects of Solid-Gas Coupling Coal-Like Materials

Quantitative simulation tests of coal and gas outbursts and CO_2 sequestration need to ensure that the coal-like material has highly consistent mechanical, deformation and gas adsorption/desorption characteristics with the natural coal [13,19–21]. In the past, such similarity was difficult to achieve [6,10,13,18,19,29], mainly because the deformation characteristics and gas adsorption/desorption characteristics were less considered. This study tested multiple indexes including the density, compressive strength, elastic modulus, cohesion, internal friction angle, porosity and gas adsorption and desorption parameters. The deformation features and damage modes of coal-like materials were also considered. Finally, samples with highly consistent stress-strain curves to the natural coal were obtained.

Since the tectonically deformed coal seam is extremely soft and fragile, it remains difficult to obtain natural coal samples that meet the test requirements and the related triaxial/long-term mechanical properties are still unclear. Existing studies have shown that the strength and deformation characteristics of reconstituted coal-like materials and natural coal were similar [20,23,27]. In view of the highly consistent mechanical properties, the homogeneity and the reproducibility of the coal-like material developed in this study; the synthetic material could be used in place of natural coal sample to study the triaxial and rheological mechanical properties of soft tectonically deformed coal. The relevant experimental results will help guide the design of roadway support for soft coal seams, the stability control of the gas drainage borehole [49,50] and the prediction of coal and gas delayed outburst.

4. Conclusions

In this study, solid-gas coupling coal-like materials were developed according to the characteristics of low strength, strong plastic deformation and large gas adsorption capacities of natural TDC. Coal powder was used as the aggregate, gypsum and petrolatum as the composite binder, calcium carbonate as the additive and vertical ground stress as the molding pressure. The orthogonal method was used to design 25 groups of material ratio schemes. The physical and mechanical parameters, deformation features and gaseous constants were obtained by carrying out uniaxial compression, variable angle shearing and gas adsorption/desorption tests. The following conclusions were obtained.

(1) The range analysis indicates that the gypsum/petrolatum ratio played the main role in controlling the sample density, compressive strength, elastic modulus, cohesion and deformation characteristic. The coarse coal powder (1–2 mm)/fine coal powder (0–0.5 mm) ratio was mainly in control of the sample internal friction angle and also had an important influence on the compressive strength and elastic modulus. When the fine coal powder/aggregate ratio was about 70%, the sample had the highest strength. With the gypsum/petrolatum ratio increasing from 5:5, 6:4, 7:3, 8:2 to 9:1, the deformation characteristics of coal-like materials transitioned from ductile to brittle; and the

failure modes included typical squeezing damage, wedge splitting, plastic shear failure, brittle shear and brittle fracturing. The content of coal powder played a decisive role in the gas adsorption and desorption characteristics of coal-like materials. An empirical formula between coal powder content and gas adsorption index was also established.

(2) The microstructures of specimens indicate that an even mixing with the cementing agent is difficult when there is a large ratio of fine coal particles, resulting in poor strength stability and low homogeneity of the sample. When the ratio of coarse/fine coal particles was about 3:7, the binder and aggregate were relatively well mixed and the specimen had a compact structure.

(3) A multivariate linear model was established between the mechanical characteristic indexes and their main influencing factors. Then, the desired material ratio was determined using this model and the developed coal-like material showed high similarity in its mechanical and physicochemical properties to the natural coal sample. Meanwhile, developing new binders that simultaneously improve sample strength and gas adsorption/desorption performance would help further reduce the difference between coal-like material and natural coal.

(4) The method for preparing solid-gas coupling coal-like material was optimized and the developed samples had good reproducibility and homogeneity. This study lays the foundation for future quantitative work in the physical simulation of coal and gas outbursts, the long-term safety study of CO_2 sequestration with coal in the lab and other experiments on the mechanical properties of soft coal seams.

Author Contributions: X.W. prepared the manuscript and conducted the investigation, Z.S. was responsible for the methodology and software, Q.T. carried out the data processing, W.X. acquired the funding and wrote, reviewed and edited the manuscript.

Funding: This research was funded by State Key Laboratory of Coal Resources and Safe Mining, China University of Mining and Technology (Grant No. SKLCRSM15X01) and National Key Research and Development Plan (Grant No. 2017YFC0603001).

Acknowledgments: We wish to thank Wanxin Song for supporting this experiment, as well as Xiaoying Fan for her great encouragement during the research process. We would like to thank Editage [www.editage.cn] for English language editing.

Conflicts of Interest: The authors declare no conflict of interest.

References

1. Valliappan, S.; Zhang, W.H. Role of gas energy during coal outbursts. *Int. J. Numer. Meth. Eng.* **1999**, *44*, 875–895. [CrossRef]
2. Lama, R.D.; Bodziony, J. Management of outburst in underground coal mines. *Int. J. Coal. Geol.* **1998**, *35*, 83–115. [CrossRef]
3. Wang, F.; Zhao, X.; Liang, Y.; Li, X.; Chen, Y. Calculation Model and Rapid Estimation Method for Coal Seam Gas Content. *Processes* **2018**, *6*, 223. [CrossRef]
4. Beamish, B.B.; Crosdale, P.J. Instantaneous outbursts in underground coal mines: An overview and association with coal type. *Int. J. Coal. Geol.* **1998**, *35*, 27–55. [CrossRef]
5. Skoczylas, N.; Dutka, B.; Sobczyk, J. Mechanical and gaseous properties of coal briquettes in terms of outburst risk. *Fuel* **2014**, *134*, 45–52. [CrossRef]
6. Zhao, B.; Wen, G.C.; Sun, H.T.; Sun, D.L.; Yang, H.M.; Cao, J.; Dai, L.C.; Wang, B. Similarity criteria and coal-like material in coal and gas outburst physical simulation. *Int. J. Coal Sci. Technol.* **2018**, *5*, 167–178. [CrossRef]
7. Chen, L.; Wang, E.Y.; Ou, J.C.; Fu, J.W. Coal and gas outburst hazards and factors of the No. B-1 Coalbed, Henan, China. *Geosci. J.* **2018**, *22*, 171–182. [CrossRef]
8. Wang, G.; Wu, M.M.; Wang, H.Y.; Huang, Q.M.; Zhong, Y. Sensitivity analysis of factors affecting coal and gas outburst based on an energy equilibrium model. *Chin. J. Rock Mech. Eng.* **2015**, *34*, 238–248. (In Chinese) [CrossRef]
9. Yuan, L. Control of coal and gas outbursts in Huainan mines in China: A review. *J. Rock Mech. Geotech. Eng.* **2016**, *8*, 559–567. [CrossRef]

10. Wang, G.; Li, W.X.; Wang, P.F.; Yang, X.X.; Zhang, S.T. Deformation and gas flow characteristics of coal-like materials under triaxial stress conditions. *Int. J. Rock Mech. Min. Sci.* **2017**, *91*, 72–80. [CrossRef]
11. Peng, S.J.; Xu, J.; Yang, H.W.; Liu, D. Experimental study on the influence mechanism of gas seepage on coal and gas outburst disaster. *Saf. Sci.* **2012**, *50*, 816–821. [CrossRef]
12. Skoczylas, N. Laboratory study of the phenomenon of methane and coal outburst. *Int. J. Rock Mech. Min. Sci.* **2012**, *55*, 102–107. [CrossRef]
13. Hu, Q.T.; Zhang, S.T.; Wen, G.C.; Dai, L.C.; Wang, B. Coal-like material for coal and gas outburst simulation tests. *Int. J. Rock Mech. Min. Sci.* **2015**, *74*, 151–156. [CrossRef]
14. Sun, H.T.; Cao, J.; Li, M.H.; Zhao, X.S.; Dai, L.C.; Sun, D.L.; Wang, B.; Zhai, B.N. Experimental Research on the Impactive Dynamic Effect of Gas-Pulverized Coal of Coal and Gas Outburst. *Energies* **2018**, *11*, 797. [CrossRef]
15. Alexeev, A.D.; Revva, V.N.; Alyshev, N.A.; Zhitlyonok, D.M. True triaxial loading apparatus and its application to coal outburst prediction. *Int. J. Coal. Geol.* **2004**, *58*, 245–250. [CrossRef]
16. Clayton, J.L. Geochemistry of coalbed gas—A review. *Int. J. Coal. Geol.* **1998**, *35*, 159–173. [CrossRef]
17. Prusty, B.K. Sorption of methane and CO_2 for enhanced coalbed methane recovery and carbon dioxide sequestration. *J. Nat. Gas Chem.* **2008**, *17*, 29–38. [CrossRef]
18. Jasinge, D.; Ranjith, P.G.; Choi, S.K.; Kodikara, J. Mechanical Properties of Reconstituted Australian Black Coal. *J. Geotech. Geoenviron. Eng.* **2009**, *135*, 980–985. [CrossRef]
19. Jasinge, D.; Ranjith, P.G.; Choi, S.K. Development of a reconstituted brown coal material using cement as a binder. *Environ. Earth Sci.* **2011**, *64*, 631–641. [CrossRef]
20. Jasinge, D.; Ranjith, P.G.; Choi, X.; Fernando, J. Investigation of the influence of coal swelling on permeability characteristics using natural brown coal and reconstituted brown coal specimens. *Energy* **2012**, *39*, 303–309. [CrossRef]
21. Ranjith, P.G.; Shao, S.S.; Viete, D.R.; Jaysinge, D. Carbon Dioxide Storage in Coal: Reconstituted Coal as a Structurally Homogeneous Substitute for Coal. *Int. J. Coal Prep. Util.* **2012**, *32*, 265–275. [CrossRef]
22. Skochinski, A.A. *Communication of the Initiation of a Sudden Outburst of Gas and Coal in the Model in Outburst Laboratory of the Institute of Mining of AN, SSSR*; Ugol: Novokuznetsk, Russia, 1953; p. 10.
23. Yin, G.Z.; Huang, Q.X.; Zhang, D.M.; Wang, D.K. Test study of gas seepage characteristics of gas-bearing coal specimen during process of deformation and failure in geostress field. *Chin. J. Rock Mech. Eng.* **2010**, *29*, 336–343. (In Chinese)
24. Jiang, C.B.; Yin, G.Z.; Li, X.Q.; Cai, B. Experimental study of gas permeability of outburst coal briquettes in complete stress-strain process. *Chin. J. Rock Mech. Eng.* **2010**, *29*, 3482–3487. (In Chinese)
25. Cao, S.G.; Li, Y.; Guo, P.; Bai, Y.J.; Liu, Y.B. Comparative research on permeability characteristics in complete stress-strain process of briquettes and coal samples. *Chin. J. Rock Mech. Eng.* **2010**, *29*, 899–906. (In Chinese)
26. Chen, H.D.; Cheng, Y.P.; Zhou, H.X.; Li, W. Damage and Permeability Development in Coal During Unloading. *Rock Mech. Rock Eng.* **2013**, *46*, 1377–1390. [CrossRef]
27. Xu, J.; Geng, J.B.; Peng, S.J.; Liu, D.; Nie, W. Acoustic emission characteristics of coal and gas outburst under different moisture contents. *J. China Coal Soc.* **2015**, *35*, 1047–1054. [CrossRef]
28. Jasinge, D.; Ranjith, P.G.; Kodikara, J.; Al, E. A Comparision of Stress Strain Behavior of Reconstituted and Natural Black Coal. In Proceedings of the Congress of the 11th ISRM of the International Society of Rock Mechanics, Lisbon, Portugal, 9–13 July 2007.
29. Xu, J.; Ye, G.B.; Li, B.B.; Cao, J.; Zhang, M. Experimental study of mechanical and permeability characteristics of moulded coals with different binder ratios. *Rock Soil Mech.* **2015**, *36*, 104–110. (In Chinese) [CrossRef]
30. Zhang, Q.H.; Yuan, L.; Wang, H.P.; Kang, J.H.; Li, S.C.; Xue, J.H.; Zhou, W.; Zhang, D.M. Establishment and analysis of similarity criteria for physical simulation of coal and gas outburst. *J. China Coal Soc.* **2016**, *41*, 2773–2779. (In Chinese) [CrossRef]
31. Zhang, S.T.; Lin, D.C.; Wang, B.; Cao, J. Experimental study of mixture ratio of similar material for simulation of coal and gas outburst. *Coal Sci. Technol.* **2015**, *43*, 76–80. (In Chinese) [CrossRef]
32. Wang, J.L.; Li, M.; Xu, S.C.; Qu, Z.H.; Jiang, B. Simulation of Ground Stress Field and Advanced Prediction of Gas Outburst Risks in the Non-Mining Area of Xinjing Mine, China. *Energies* **2018**, *11*, 1285. [CrossRef]
33. Yin, W.T.; Fu, G.; Yang, C.; Jiang, Z.G.; Zhu, K.; Gao, Y. Fatal gas explosion accidents on Chinese coal mines and the characteristics of unsafe behaviors: 2000–2014. *Saf. Sci.* **2017**, *92*, 173–179. [CrossRef]

34. Wang, C.J.; Yang, S.Q.; Yang, D.D.; Li, X.W.; Jiang, C.L. Experimental analysis of the intensity and evolution of coal and gas outbursts. *Fuel* **2018**, *226*, 252–262. [CrossRef]
35. Li, H.Y. Major and minor structural features of a bedding shear zone along a coal seam and related gas outburst, Pingdingshan coalfield, northern China. *Int. J. Coal. Geol.* **2001**, *47*, 101–113. [CrossRef]
36. Cao, Y.X.; Mitchell, G.D.; Davis, A.; Wang, D.M. Deformation metamorphism of bituminous and anthracite coals from China. *Int. J. Coal. Geol.* **2000**, *43*, 227–242. [CrossRef]
37. Ju, Y.W.; Jiang, B.; Hou, Q.L.; Tan, Y.J.; Wang, G.L.; Xiao, W.J. Behavior and mechanism of the adsorption/desorption of tectonically deformed coals. *Chin. Sci. Bull.* **2009**, *54*, 88–94. [CrossRef]
38. Ju, Y.W.; Jiang, B.; Hou, Q.L.; Wang, G.L. The new structure-genetic classification system in tectonically deformed coals and its gelological significance. *J. China Coal Soc.* **2004**, *29*, 513–517. (In Chinese) [CrossRef]
39. China National Coal Association. *Methods for Determining the Physical and Mechanical Properties of Coal and Rock—Part 7: Methods for Determining the Uniaxial Compressive Strength and Counting Softening Coefficient*; GB/T 23561.7-2009; China National Coal Association: Beijing, China, 2009.
40. China National Coal Association. *Methods for Determining the Physical and Mechanical Properties of Coal and Rock—Part 11: Methods for Determining Shear Strength of Coal and Rock*; GB/T 23561.11-2010; China National Coal Association: Beijing, China, 2010.
41. Mansouri, H.; Ajalloeian, R. Mechanical behavior of salt rock under uniaxial compression and creep tests. *Int. J. Rock Mech. Min. Sci.* **2018**, *110*, 19–27. [CrossRef]
42. Gao, Y.J. Analysis of the Factors Influencing Briquette Forming and Design of Roll Briquetting Machine. Master's Thesis, Shanxi University, Taiyuan, China, 2009. (In Chinese with English abstract).
43. Liu, S.; Liu, W. Experimental Development Process of a New Fluid–Solid Coupling Similar-Material Based on the Orthogonal Test. *Processes* **2018**, *6*, 211. [CrossRef]
44. Brown, E.T. *Suggested Method for Determining the Uniaxial Compressive Strength of Rock Materials, Rock Characterization, Testing and Monitoring*; ISRM Suggested Methods; Pergamon Press: Oxford, UK, 1981.
45. Yang, D.D.; Chen, Y.J.; Tang, J.; Li, X.W.; Jiang, C.L.; Wang, C.J.; Zhang, C.J. Experimental research into the relationship between initial gas release and coal-gas outbursts. *J. Nat. Gas Sci. Eng.* **2018**, *50*, 157–165. [CrossRef]
46. Laxminarayana, C.; Crosdale, P.J. Role of coal type and rank on methane sorption characteristics of Bowen Basin, Australia coals. *Int. J. Coal. Geol.* **1999**, *40*, 309–325. [CrossRef]
47. Ruppel, T.C.; Grein, C.T.; Bienstock, D. Adsorption of methane on dry coal at elecated pressure. *Fuel* **1974**, *53*, 152–162. [CrossRef]
48. Jasinge, D.; Ranjith, P.G.; Choi, S.K. Effects of effective stress changes on permeability of latrobe valley brown coal. *Fuel* **2011**, *90*, 1292–1300. [CrossRef]
49. Tang, J.; Jiang, C.L.; Chen, Y.J.; Li, X.W.; Wang, G.D.; Yang, D.D. Line prediction technology for forecasting coal and gas outbursts during coal roadway tunnelling. *J. Nat. Gas Sci. Eng.* **2016**, *34*, 412–418. [CrossRef]
50. Xue, Y.; Gao, F.; Gao, Y.; Chen, H.M.; Liu, Y.K.; Hou, P.; Teng, T. Quantitative evaluation of stress-relief and permeability-increasing effects of overlying coal seams for coal mine methane drainage in Wulan coal mine. *J. Nat. Gas Sci. Eng.* **2016**, *32*, 122–137. [CrossRef]